



UNIVERSITY OF LEEDS

This is a repository copy of *Hydrogen Bubble Growth and Release Dynamics in Glass Bead Beds for Applications in Legacy Nuclear Waste – 24256*.

White Rose Research Online URL for this paper:

<https://eprints.whiterose.ac.uk/212357/>

Version: Accepted Version

Proceedings Paper:

Sibanda, G.A., Fairweather, M., Peakall, J. et al. (4 more authors) (2024) Hydrogen Bubble Growth and Release Dynamics in Glass Bead Beds for Applications in Legacy Nuclear Waste – 24256. In: WM2024 Conference Proceedings. WM Symposia 2024, 2024-03-10 2024-03-14, Phoenix, AZ, USA. WM Symposia .

© 2024 WM Symposia. This is an author produced version of a conference paper accepted for publication in WM2024 Conference Proceedings. Uploaded with permission from the copyright holder.

Reuse

Items deposited in White Rose Research Online are protected by copyright, with all rights reserved unless indicated otherwise. They may be downloaded and/or printed for private study, or other acts as permitted by national copyright laws. The publisher or other rights holders may allow further reproduction and re-use of the full text version. This is indicated by the licence information on the White Rose Research Online record for the item.

Takedown

If you consider content in White Rose Research Online to be in breach of UK law, please notify us by emailing eprints@whiterose.ac.uk including the URL of the record and the reason for the withdrawal request.



eprints@whiterose.ac.uk
<https://eprints.whiterose.ac.uk/>

Hydrogen Bubble Growth and Release Dynamics in Glass Bead Beds for Applications in Legacy Nuclear Waste – 24256

Gamuchirai Ashley Sibanda¹, Michael Fairweather², Jeffrey Peakall², David Harbottle², Martyn Barnes³, Alice Macente⁴ and Timothy Hunter²

¹School of Chemical and Process Engineering University of Leeds

²School of Earth and Environment University of Leeds

³Sellafield Ltd, Hinton House, Birchwood Park Ave, Birchwood

⁴School of Civil Engineering University of Leeds

ABSTRACT

For the planning and design of long-term storage facilities and the monitoring of interim waste storage, a thorough comprehension of the gaseous release is required. A build-up of gases such as hydrogen, underscores the importance of studying these dynamics for interim and geological disposal facility (GDF) safety cases. The UK Radioactive Waste Management (RWM) organization estimates around 103 000 tons of metals that are categorized as GDF waste. The volume of hydrogen gas from radiolysis and/or corrosion that is trapped in interim waste storage facilities is unknown. This uncertainty and continuous gas release needs to be considered in the design of containers for radioactive waste storage. Gas transport occurs via capillary invasion or sediment fracturing. Bubbles in sediments with low yield stress may fail to invade or fracture these sediments resulting in gas build-up. Over-estimation of hydrogen hold-up per waste material will result in high mobilization and storage costs hence the need for a greater understanding of bubble dynamics and sediment mechanics.

This work uses silica glass beads to simulate characteristics of granular nuclear waste. Hydrogen is generated from induced magnesium corrosion in columns packed with glass beads. Sodium chloride was added to catalyze corrosion by disturbing the protective magnesium hydroxide layer that forms in room temperature water. Four sizes of glass beads 88 μm , 203 μm , 394 μm and 555 μm were used to see the effects of particle size and yield stress on hydrogen generation rates, bubble sizes and overall release versus retention rates. Hydrogen retention and bed expansion were found to increase with decreasing particle size. Smaller particles had higher total hydrogen yield except for the 88 μm which had large gas pockets. Gas transport by invasion increased with increasing particle sizes which had higher yield stress values.

Samples are imaged using high resolution X-ray Computed Tomography to study the microstructure and bubble distribution. A sample of hydrogen bubbles in glass beads of mean size 203 μm , was imaged with a pixel size of 53 μm and showed coalescence of bubbles at the edges of the sample from the wall effects. The contribution from micro and macro bubble pores will be evaluated after selecting an effective region of interest (ROI) and a gas network model will be developed from this. Over time, the glass beads show plasticity after bubble formation like other granular materials such as sand, which tend to have spherical bubbles. This project is in partnership with Sellafield Ltd.

INTRODUCTION

Sellafield Ltd has been storing magnesium cladding waste in the Magnox swarf storage silo (MSSS) since 1964 [1]. Over decades, this waste has corroded resulting in continuous hydrogen production in the silo which has a complex composition of sludge and some solid material. The large volumes make this one of

the most hazardous waste facilities in the UK. Depth dependent waste characterization of the waste in the silos is needed for the planning of removal techniques and for the design and quantification of storage boxes. Concerns with gas generation expand to include other forms of consolidated waste such as the zeolite ion exchange material which has been used to remove harmful elements like strontium and cesium from nuclear waste. The exposure to radiation in these ion exchange processes leads to radiolysis which produces hydrogen. Over the decades that these plants have been in operation, large volumes of this granular, gas generating waste have accumulated. Understanding the rates of gas generation and gas retention in sludges and granular sediments will better inform safety and economic factors for decommissioning.

Factors such as yield stress will affect the volumes of trapped gas. Low yield stress sediments will be more likely to expand as gas is generated. As illustrated in Figure 1, gas in 3-phase systems can escape either by capillary invasion when the capillary pressure is great enough relative to the pore entry pressure or by sediment fracturing when this pore entry pressure is too high for invasion forming cracks through which gas can continuously be released [2]. Some sediments can be said to have elastic properties by which the solid particles can return to their position after being displaced or fractured. These elastic properties lead to some sediments having steady gas release while some have abrupt high gas release. In granular material, capillary forces and gravitational forces govern the displacement capacity. Altering the surface properties like hydrophobicity by coating particles will change the liquid contact angles affecting the surface tension effects on cohesive forces. This can be achieved by adjusting the ion composition of the liquid phase or by esterifying the particles. Ion concentrations affect the particle layer, and these changes can be quantified by zeta-potential measurements which should result in variance in the yield stress. Yamaguchi *et al.* [3] found that increasing the absolute zeta potential of silica particles lowered the yield stress relative to the pH. All these interactions and forces are size dependent. Jain and Juanes [2] found the particle size to have the greatest effect on the gas release dynamics. This project investigates this by using silica glass beads of different sizes focusing on the hydrogen gas transport mechanisms and the generation rates. The effects of physical properties of granular materials on factors such as bubble shapes, pore connectivity, depth dependence and overall volumes are not well understood. A comprehensive study of these factors in different systems will help predict long-term gas behavior and sediment expansion.

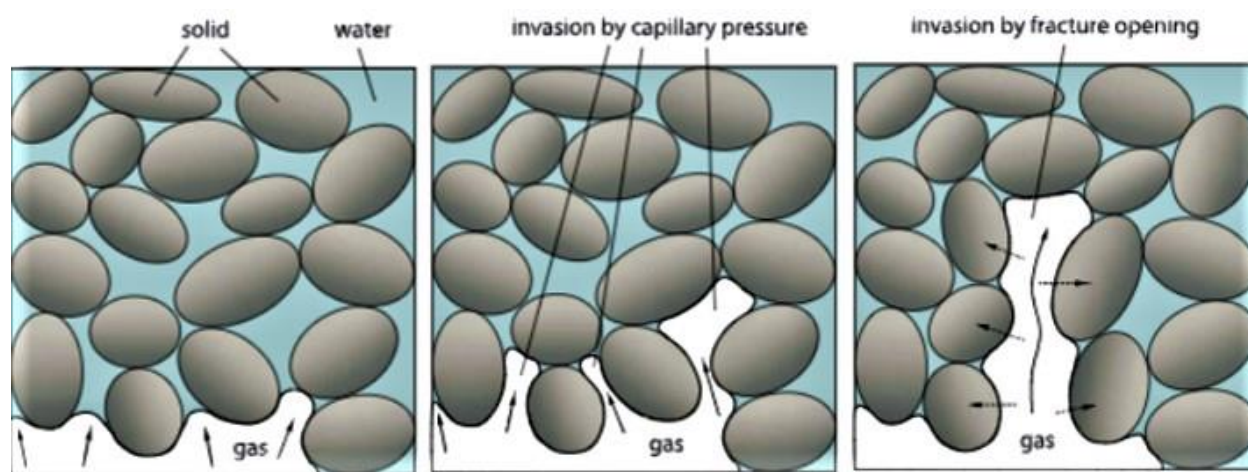


Figure 1. Mechanisms of gas movement in sediments. Reproduced with permission from [2]

Hydrogen is generated in the Magnox silo from corrosion and radiolysis. This work studies magnesium corrosion effects. Magnesium is unreactive in water at room temperatures. A protective hydroxide layer

forms on the surface prohibiting corrosion. Reducing the pH by adding acids can prolong the hydroxide layer formation until passivation occurs at approximately pH 9. Alternatively, ions from salts can disrupt the hydroxide layer leading to pitting corrosion which will allow corrosion to occur for longer periods and can be adjusted to vary the rates or reaction [4]. The corrosion rate affects the retention capacity of the sediment. Visual analysis of gas in glass beads samples with X-ray Computed Tomography (XCT) imaging shows the distribution of the bubbles and the contribution of different sizes to the total gas volumes. Permeability constants can be estimated from the XCT images using Monte Carlo and Lattice Boltzmann (LBM) techniques. LBM is a mesoscopic technique. Micropores can be incorporated using pore network models for more accurate estimations. Rabbani *et al.* [5] have developed a triple-pore network model (T-pnm) which models micro and meso-pores with pore throat radii and fracture paths. Data from imaging hydrogen in glass beads of different sizes and different generation rates can be used as inputs for some of the models and to visualize the preferred gas transport patterns.

MATERIALS AND METHODS

Materials

Table 1. Materials and Specifications

Material	Specifications and Suppliers
Honite (silica glass beads)	Guyson International Ltd, UK Honite 8 : 425 – 600 μm Honite 9 : 250 – 425 μm Honite 12 : 150 – 250 μm Honite 16 : 53 – 106 μm
Magnesium powder	Alfa Aesar, USA, -325 mesh, 99.8 %
Sodium chloride	Avantor, UK, Baker analyzed reagent, general lab reagent

Sediment Characterization

Samples of four different glass bead grades were sized using a Mastersizer 3000 (Malvern Panalytical Ltd, UK). The natural consolidation point of samples was estimated by adding different amounts of glass beads in water and calculating the end volume fractions. At the natural consolidation point, the final volume fraction will stop changing drastically. Samples between 6 and 25 wt% were put in measuring cylinders and shaken then left to settle. The yield stress of the beads in water was calculated from torque percentages measured by a viscometer (Brookfield AMETEK, USA). Vanes with a cylindrical arrangement were used for these measurements. The shear yield stress measurements calculated from the torque values were plotted

against the volume fractions to study the rate of increase in yield stress as the volume fraction increased which will influence the bubble evolution behavior and the gas release dynamics.

Gas Generation

Hydrogen production is simulated via magnesium powder corrosion. The set-up in Figure 2 was recorded by a camera and volumes at selected time intervals were obtained from the recordings. The water level in the inverted cylinder was recorded as well as the water level above the glass bead bed and the level of the top solid layer. The difference in start and end water levels above the glass bead bed was taken to be the retained gas and the change in solid bed height was the bed expansion. The total generated gas volume was calculated as the sum of the retained gas and the volume of gas displacing water in the inverted cylinder (released). From the consolidation tests, the glass beads were found to have a natural consolidation point at around 60 vol% so 897 g of glass beads were added to a mixture of 224 ml deionized water, 25.3 g of sodium chloride (2 wt%) and 4 g of magnesium. The magnesium was left to corrode for 24 hours and experiments were repeated for different bead sizes (average sizes of 555 μm , 394 μm , 203 μm and 88 μm).

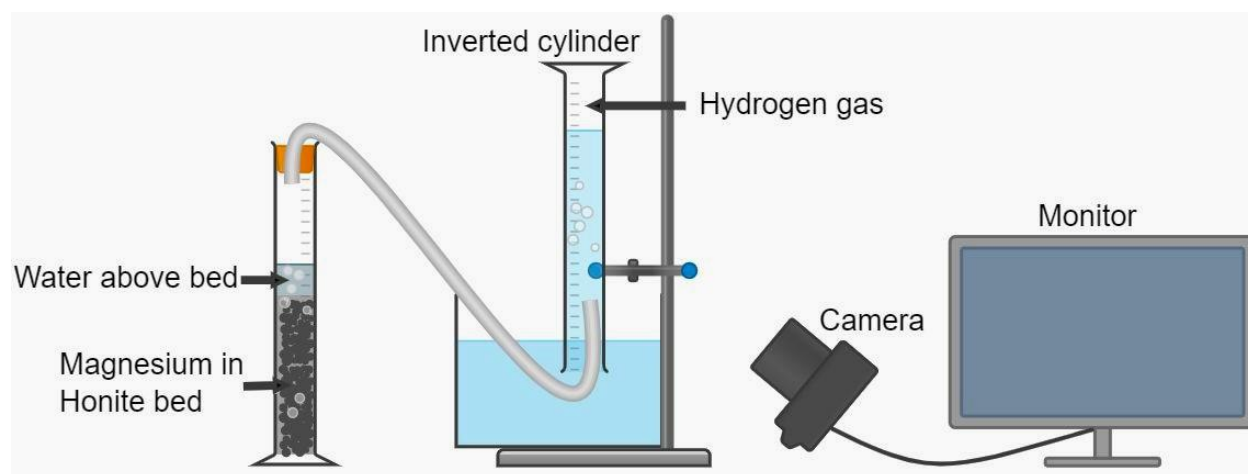


Figure 2. Experimental set-up of hydrogen gas hold-up in glass beads.

XCT Imaging

Samples of hydrogen bubbles dispersed in glass beads are imaged using a high-resolution X-ray CT scanner at a final reconstructed pixel size of 53 μm (ZEISS Xradia 410 Versa). The high-resolution scanner gives detailed information on the micro-bubble distribution, but the small sample size required (4 cm diameter, 4 cm height cylindrical tube) results in significant wall effects. This can be resolved by choosing a central region of interest or by using larger samples with a lower resolution scanner which shows the macro-bubbles with reduced wall effects. Due to the sensitivity of the high-resolution CT scanner to movement within the sample, the smaller samples are only scanned after the 24-hour period to look at the final bubble distribution. High resolution scanning will help to look at pore connections. Post-processing was done in Fiji ImageJ and MATLAB for analysis of bubble size distributions. Sample compositions were scaled relative to the experimental values.

RESULTS AND DISCUSSION

Sediment Characterization

Table 2 shows the mean values for the glass bead sizes. The coefficient of variation increases with decreasing mean particle size which indicates that the larger particle samples have more homogeneity and less fines. This was confirmed with SEM images as in Figure 3 which show majority uniform sphericity with some minor manufacturing defects. The yield stress decreased with decreasing particle size (also Table 2). This confirms yield stress dependence on particle size and not just volume fraction. Johnson *et al.* [6] found that high yield stress results in more bubble invasion between the particles and less overall retention so the largest particle size may have the least volume of hydrogen retained due to this factor. Smaller particles can still have high rates of gas release from the capillary pressure [3]. The gas hold-up experiments investigate the overall effects of the combined factors.

Table 2. Percentages of Hydrogen retained in the bed and the bed expansion.

Log mean (μm) +/- one standard deviation	Coefficient of variation (%)	Yield stress (Pa) +/- one standard deviation
555 +/- 0.186	0.0272	163 +/- 17.1
394 +/- 0.392	0.0472	97.3 +/- 14.7
203 +/- 0.0164	0.0773	64.1 +/- 11.3
88 +/- 0.129	0.231	51.5 +/- 9.39

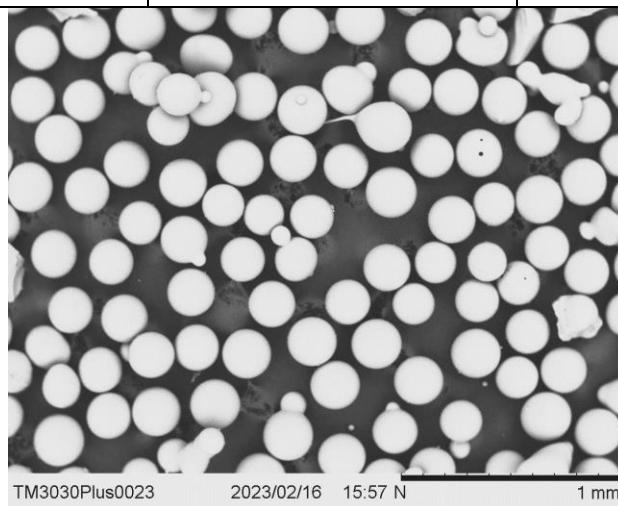


Figure 3. SEM image of 203 μm glass beads.

Gas hold-up

After about 6 hours, the gas generation passivates in the glass bead columns compared to corrosion without glass beads as in Figures 5 and 6. Without glass the corrosion continues at a relatively steady rate after the 24-hour testing period. This may be due to the mixing of the magnesium particles in solution with reduced exposure to the liquid phase in the packed columns as well as the displacement of the water as it is moved above the solid bed by the gas trying to escape the column. Figure 5 shows that the total gas generated decreases with increasing glass bead size as the surface area increases. This is except for the smallest size of 88 μm which has the same gas yield as the largest size. It may be expected that, as the surface area to volume ratio increases with decreasing particle size, hydrogen gas production may become more catalyzed, leading to the observed increases. However, for the smallest particles, the capillary space is reduced to a level that significantly limits gas production. Indeed, as shown in Figure 7, at 88 μm , the gravitational and capillary forces are such that the particles are easily displaced by the gas producing the large void spaces. The corrosion rate could be varied by reducing the concentration of magnesium and sodium chloride. In Figure 6, the rate depends on the sodium chloride catalyst concentration, though this effect is reduced at high concentrations. At high concentrations, the generation is more comparable to initial waste corrosion rates. Lower rates are required for comparison to the behavior after decades and for future predictions.

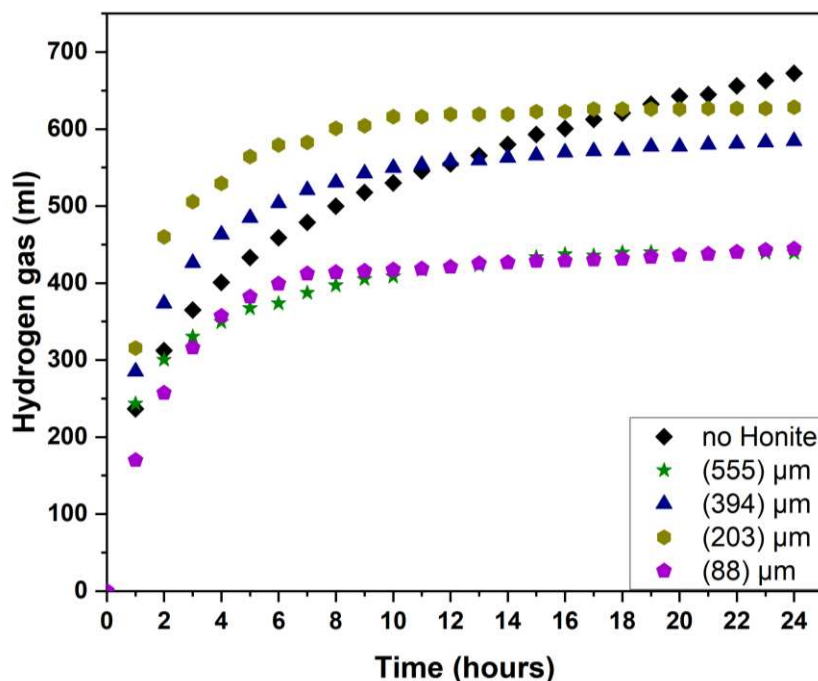


Figure 5. Hydrogen gas generation in columns of different glass bead sizes (555 μm , 394 μm , 203 μm and 88 μm mean sizes).

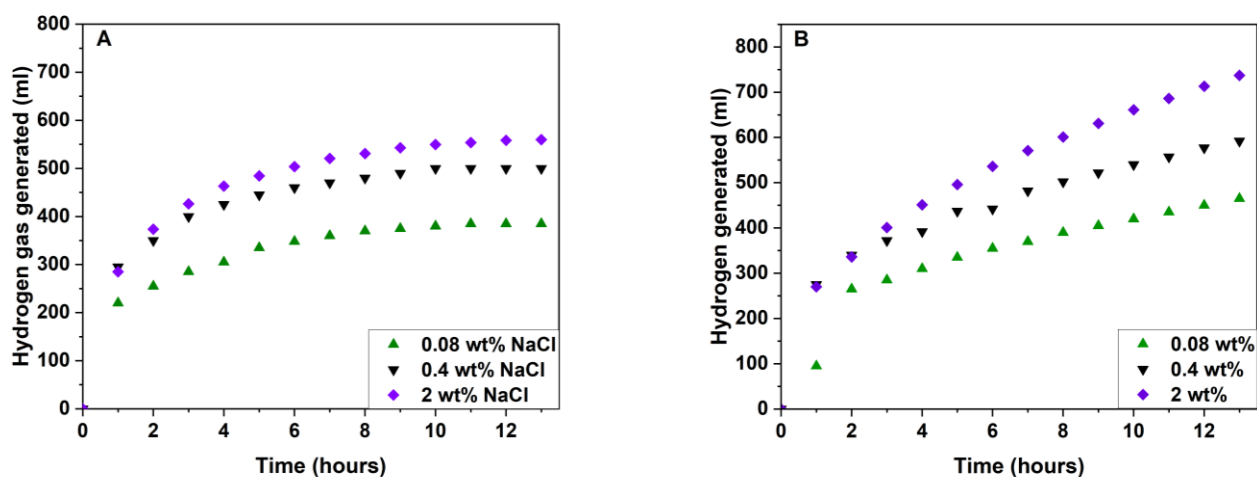


Figure 6: Effects of sodium chloride concentration on magnesium corrosion in a glass bead column of 394 μm (A) and without glass beads (B)

The retention percentages in Table 3 show that the larger bead sizes retained less hydrogen with as high as 42 % retained in the 88 μm column. This supports the trend of increased gas release with higher yield stress reported by Johnson *et al.* [6]. The transport mechanism by which this is achieved can be derived from CT images of bubble distributions in different particle sizes. The smaller particles experience more bed expansion as the gas pores get larger but there is insufficient pressure to form fractures resulting in the large voids in Figure 7 which remain stagnant unless the column is mechanically perturbed. These large voids lead to an overestimation in bed expansion as this is mostly due to wall effects from the diameter of the column used. A larger vessel would have less bed expansion as shown by the large standard deviation at 555 μm when this was tested with a wider vessel.

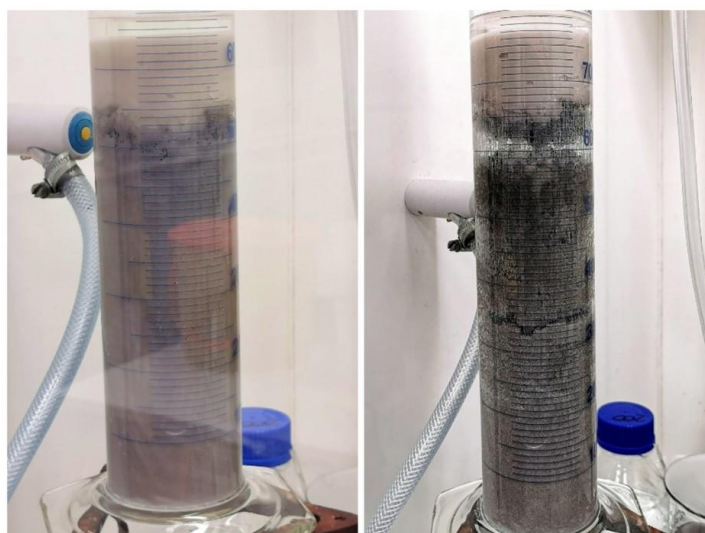


Figure 7. Images of a column with glass beads of 88 μm average size at time $t = 0$ hours (left) and time $t = 24$ hours (right).

Table 3. Percentages of Hydrogen retained in the bed and the bed expansion.

Glass beads mean size (μm)	% Hydrogen retained	% Bed expansion +/- one standard deviation
555	14.9 +/- 4.4	8 +/- 8
394	16.8 +/- 7.4	10 +/- 2.2
203	17.2 +/- 1.9	17 +/- 1.3
88	42.1 +/- 3.3	29 +/- 8

XCT Imaging

A small (4 cm diameter, 3 cm height) sample of hydrogen bubbles in 203 μm imaged at 53 μm per pixel shows the wall effects as in Figure 8. A region of interest (ROI) in the center of these images can be extracted to focus more on the meso-pores. Object counting in 3-D can give the sizes of individual bubbles as in Figure 8 (right). The number of bubbles and size range will depend on the ROI selected. The selection in Figure 8 has over 700 bubbles from the set threshold. The bubbles in the ROI are relatively spherical while the bubbles closer to the wall tend to coalesce resulting in larger voids. As shown in Figure 1, granular material can yield to encompass spherical bubbles which Boudreau *et al.* [8] found when comparing sand to mud; the granular material had some plasticity which resulted in spherical bubbles as opposed to the disk-like shape in the mud.

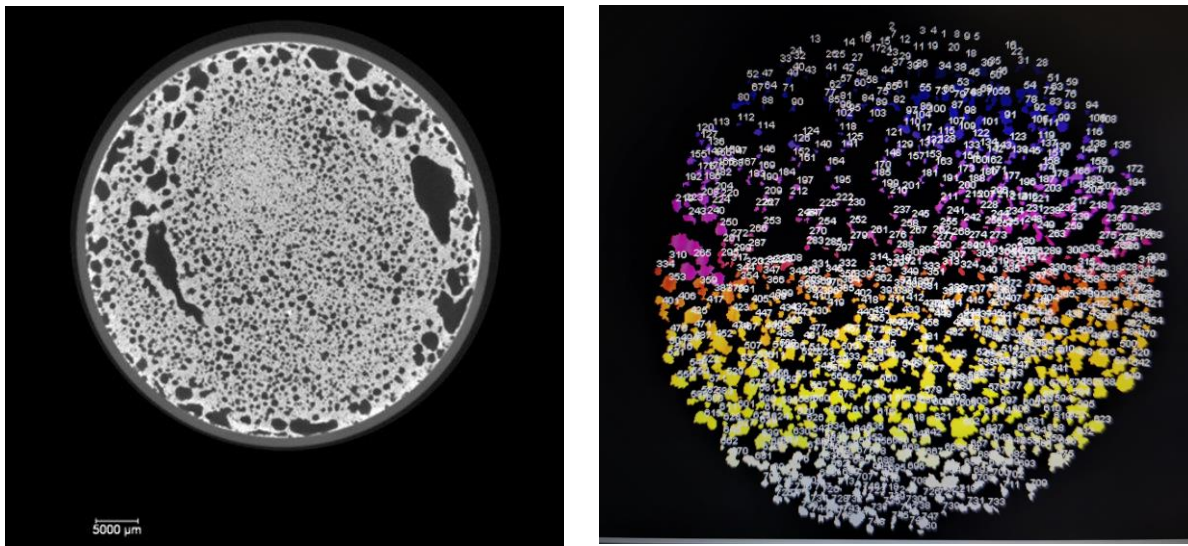


Figure 8. X-Ray Images of hydrogen bubbles in a sample bed with mean bead size of 203 μm . XY plane (left) and numbered bubbles from a selected ROI (right).

CONCLUSION

Reproducible hydrogen generation in silica glass bead columns has been established via sodium chloride induced magnesium corrosion in water. The generation rate and total yield is dependent on the particle size and ionic composition of the solution. The smaller the size, the more hydrogen is produced and the greater the percentage yield retained in the column. Particle size and yield stress affect the bubble size and distribution in granular materials. The decrease in particle size and wall effects result in the large void formation. Future work will look to reduce the wall effects and reduce the corrosion rate to see the effect of rate on retention capacity and to compare to the lower, steady generation rates in the nuclear waste silos. The effects of surface properties relative to size will be investigated by coating the silica beads. Post-processing of XCT images will be done to get pore throat radii and bubbles shapes in terms of sphericity. Low- and high-resolution XCT images will be combined to form network models and estimate permeability. Rate constants can be calculated from the experimental hydrogen production rates. Analysis of the magnesium particles for corrosion patterns may also give indications for long-term behavior.

REFERENCES

1. Inventory for geological disposal Differences Report (2021). *NDA*. url: <https://rwm.nda.gov.uk> (visited on 01/18/2022)
2. A. K. JAIN and R. JUANES, “Preferential Mode of gas invasion in sediments: Grain-scale mechanistic model of coupled multiphase fluid flow and sediment mechanics,” *Geophys Res*, 114, B8.B08101, (2009).
3. A. YAMAGUCHI, M. KOBAYASHI, Y. ADACHI, “Yield stress of mixed suspension of silica particles and lysozymes: The effect of zeta potential and adsorbed amount,” *Colloids and Surfaces A: Physicochemical and Engineering Aspects*, 578, (2019).
4. M. RASHAD, F. PAN, M. ASIF and X. CHEN, “Corrosion behavior of magnesium-graphene composites in sodium chloride solutions,” *Magnesium and Alloys*, 5, 3, (2017).
5. A. RABBANI, M. BABAEI, F. JAVADPOUR, “A Triple Pore Network Model (T-PNM) for Gas Flow Simulation in Fractured, Micro-porous and Meso-porous Media,” *Transport in Porous Media*, 132, (2020).
6. M. JOHNSON, D/ HARBOTTLE, M. FAIRWEATHER, T. HUNTER, J. PEAKALL, and S. BIGGS, “Yield stress dependency on the evolution of bubble populations generated in consolidated soft sediments,” *Alche*, 63, 9, (2017).
7. UK Radioactive Waste Inventory Poyry Energy Ltd and Wood Nuclear Ltd (2019). *NDA*. url:<https://ukinventory.nda.gov.uk/> (visited on 01/18/2022)
8. B. P. BOUDREAU, C. ALGAR, B. D. JOHNSON, I. CROUDACE, A. REED, Y. FURUKAWA, K. M. DORGAN, P. A. JUMARS, A. S. GRADER, B .S. GARDINER, “Bubble growth and rise in soft sediments,” *Geology*, 33, 6, (2005).

ACKNOWLEDGMENTS

This work was funded by the Engineering and Physical Sciences Research Council (EPSRC) UK, and Sellafield Ltd, through the Nuclear Energy GREEN CDT (EP/S022295/1). The authors also acknowledge Alice Macente and the *Centre for Infrastructure Materials*, University of Leeds, a UKCRIC Research Facility (EP/P017169/1) for access and support with the micro-CT experiments.